International Journal of Astrobiology (2025), **24**, e1, 1–12
doi:10.1017/S1473550425000011

CAMBRIDGE UNIVERSITY PRESS

RESEARCH ARTICLE

Submicron-scale detection of microbes and smectite from the interior of a Mars-analogue basalt sample by optical-photothermal infrared spectroscopy

Yohey Suzuki[1*], Mariko Koduka[1*], Frank E. Brenker[2,3], Tim Brooks[4], Mihaela Glamoclija[5], Heather V. Graham[6], Thomas L. Kieft[7], Francis M. McCubbin[8], Mark A. Sephton[9] and Mark A. van Zuilen[10†]

[1]Department of Earth and Planetary Science, Graduate School of Science, The University of Tokyo, Tokyo, Japan
[2]Department of Geoscience, Goethe University, Frankfurt, Germany
[3]Schwiete Cosmochemistry Laboratory, Department of Geoscience, Goethe University, Frankfurt, Germany
[4]Rare & Imported Pathogens Laboratory, UK Health Security Agency, Porton Down, Salisbury SP4 0JG, UK
[5]Department of Earth and Environmental Sciences, Rutgers University, Newark, NJ, USA
[6]NASA Goddard Space Flight Center, Astrochemistry Laboratory, Greenbelt, MD, USA
[7]Biology Department, New Mexico Institute of Mining and Technology, Socorro, NM, USA
[8]Astromaterials Research & Exploration Science Division, NASA Johnson Space Center, Houston, TX 77058, USA
[9]Department of Earth Science & Engineering, Imperial College London, London, UK
[10]CNRS-UMR6538 Laboratoire Geo-Ocean, Institut Universitaire Européen de la Mer, Université de Bretagne Occidentale, Plouzané, France
Corresponding author: Yohey Suzuki; Email: yohey-suzuki@eps.s.u-tokyo.ac.jp

Received: 17 December 2023; **Revised:** 23 December 2024; **Accepted:** 7 January 2025

Keyword: Backward planetary protection, clay-bearing rock fractures, Fourier-transform infrared (FT-IR) microscopy, in-situ single-cell detection, optical-photothermal infrared spectroscopy (O-PTIR)

Abstract

For near-future missions planed for Mars Sample Return (MSR), an international working group organized by the Committee on Space Research (COSPAR) developed the sample safety assessment framework (SSAF). For the SSAF, analytical instruments were selected by taking the practical limitations of hosting them within a facility with the highest level of biosafety precautions (biosafety level 4) and the precious nature of returned samples into account. To prepare for MSR, analytical instruments of high sensitivity need to be tested on effective Mars analogue materials. As an analogue material, we selected a rock core of basalt, a prominent rock type on the Martian surface. Two basalt samples with aqueous alteration cached in Jezero crater by the Perseverance rover are planned to be returned to Earth. Our previously published analytical procedures using destructive but spatially sensitive instruments such as nanoscale secondary ion mass spectrometry (NanoSIMS) and transmission electron microscopy coupled to energy-dispersive spectroscopy revealed microbial colonization at clay-filled fractures. With an aim to test the capability of an analytical instrument listed in SSAF, we now extend that work to conventional Fourier transform infrared (FT-IR) microscopy with a spatial resolution of 10 μm. Although Fe-rich smectite called nontronite was identified after crushing some portion of the rock core sample into powder, the application of conventional FT-IR microscopy is limited to a sample thickness of <30 μm. In order to obtain IR-based spectra without destructive preparation, a new technique called optical-photothermal infrared (O-PTIR) spectroscopy with a spatial resolution of 0.5 μm was applied to a 100 μm thick section of the rock core. By O-PTIR spectroscopic analysis of the clay-filled fracture, we obtained in-situ spectra diagnostic to microbial cells, consistent with our previously published data obtained by NanoSIMS. In addition, nontronite identification was also possible by O-PTIR spectroscopic analysis. From these results, O-PTIR spectroscopy is suggested be superior to deep

*These authors contributed equally: Yohey Suzuki, Mariko Kouduka.
†Present address: Naturalis Biodiversity Center, Leiden, The Netherlands.

ultraviolet fluorescence microscopy/μ-Raman spectroscopy, particularly for smectite identification. A simultaneous acquisition of the spatial distribution of structural motifs associated with biomolecules and smectites is critical for distinguishing biological material in samples as well as characterizing an abiotic background.

Contents

Introduction

Mars Sample Return (MSR) is a mission defined as '*Category V restricted Earth return*' by the Committee on Space Research's (COSPAR) Planetary Protection Policy (https://cosparhq.cnes.fr/scientific-structure/panels/panel-on-planetary-protection-ppp/). To cover the category description element in the policy stating a need to conduct timely analyses of any unsterilized sample collected and returned to Earth, under strict containment, and using the most sensitive techniques, an international working group was organized by COSPAR and the sample safety assessment framework (SSAF) was developed (Kminek *et al.*, 2022a).

The SSAF targets living organisms, their resting states (e.g. spores, cysts), or their remains in Martian materials. The tentative level of safety assurance is a risk value of 1 in a million chance of failing to detect life, if it is present. The risk value is estimated by Bayesian statics that takes the likelihood of samples and subsamples containing life and the sensitivity of analytical methods into consideration for the generation of probabilities. To reduce the number and volume of samples to be consumed for planetary protection, a subsampling procedure is employed. The SSAF identified optimal subsampling targets to be regions of rock samples with high concentrations of pore-spaces or fractures. As life is likely to be detected where the prolonged presence of water has formed clays by rock–water interactions, rock samples containing clays are prioritized as subsampling targets. Subsamples are subjected to a test sequence, in which non-destructive analytical steps are followed by destructive analytical steps.

Implementation of the SSAF poses challenges because most of the investigations need to be conducted within biological containment. The SSAF is therefore described at a level of detail that will support planning activities for sample receiving facilities (SRF). Three major open issues were raised to effectively implement and optimize the SSAF, specifically the need to: (1) set a level of assurance to exclude the presence of Martian life in the samples, (2) carry out an analogue test programme, and (3) acquire relevant contamination knowledge from flight and ground elements. In the analogue test programme, analytical steps need to be validated by testing with analogue samples potentially returned from Mars. In the lists of analytical instruments for SRF, Fourier-transform infrared (FT-IR) spectroscopy is requested from both the SSAF and Mars Sample Return Science Planning Group 2 (MSPG2) (Carrier *et al.*, 2022; Haltigin *et al.*, 2022; Meyer *et al.*, 2022; Tait *et al.*, 2022;

https://doi.org/10.1017/S1473550425000011 Published online by Cambridge University Press

Tosca *et al*., 2022; Velbel *et al*., 2022; Kminek *et al*., 2022b). FT-IR spectroscopy has the capability of identifying inorganic and organic materials. However, a spatial resolution of FT-IR microscopy is limited by the diffraction limit of IR light (~10 μm), which hinders the single-cell sensitivity for many microorganisms.

Optical-photothermal infrared (O-PTIR) spectroscopy has a superior spatial resolution (~0.5 μm) to FT-IR microscopy, because light scattering caused by thermal expansion under pulsed IR light with a beam diameter of ~10 μm is detected by a green laser (532 nm) with a beam diameter of ~0.5 μm and a photodiode (Li *et al*., 2019; Lima *et al*., 2021). Light-scattering response is monitored during tuning the wavenumber of the IR source, which creates a FT-IR like spectrum. In addition to the spatial superiority, O-PTIR needs no preparation steps required for FT-IR microscopy. In this study, O-PTIR spectroscopy was applied to a rock core sample where the dense colonization of microbes has been demonstrated in clay-filled fractures as an analogue for MSR (Suzuki *et al*., 2020).

Methods

Sampling and sample preparations

The rock core sample coded as U1365E-8R4 (109.6 m below the seafloor) was obtained by drilling of the 104-million-year-old basaltic basement during Integrated Ocean Drilling Project (IODP) expedition #329. IODP expedition #329 targeted life beneath the seafloor of the South Pacific Gyre (SPG), where surface photosynthetic activity is exceedingly low (D'hondt *et al*., 2015). This ultra-oligotrophic feature favours microorganisms living independently from photosynthetic organics (Morono *et al*., 2020). This feature appears to be analogous to the Martian surface, because the growth of photosynthetic organisms is likely suppressed under frozen and/or arid conditions (Onstott *et al*., 2019).

Sample preparations for the rock core sample were previously reported (Sueoka *et al*., 2019). After the recovery of the rock core sample, the contaminated exterior of the rock core sample was removed by a sterilized hammer and chisel until fluorescent microspheres present in the drilling fluids were undetected from the interior of the rock core sample by a UV fluorescent microscope. A portion of the rock interior was ground into powder by a sterilized mortar and pestle. A clay-sized fraction was separated by suspending the powder sample in deionized water, from which a fraction larger than the clay-sized fraction was removed by centrifugation at 3000 rpm for 5 min. After the separation, the supernatant was freeze-dried and stored at −30°C. For the preparation of a 100 μm thin section, a fracture-bearing rock piece was embedded in LR White resin (London Resin Co. Ltd., Aldermaston, England) and then thinned by polishing with corundum powder and diamond paste. All laboratory woks were performed in a clean bench with sterilized apparatus and reagents.

Conventional FT-IR microscopy

The clay-sized fraction in the powder sample was mounted on a diamond cell (Diamond EX'Press II, S.T. Japan Inc.). FT-IR spectra from 700 to 4000 cm^{-1} were obtained from a 10 μm square region by a Shimadzu AIM-9000 FT-IR microscope in combination with an IRTracer-100 (Cassegrain 15 × objective). A transmission mode was used with a spectral resolution of 0.25 cm^{-1}. Clay Science Society of Japan (JCSS) reference clay samples such as montmorillonite JCSS3101 ($(M+_{.97})[Si_{7.8}Al_{.02}][Al_{3.3}$-$Fe_{-.2}Mg_{.6}]O_{20}(OH)_4$) and saponite JCSS3501 ($(M+_{.98})[Si_{7.2}Al_{.08}][Mg_{6.0}]O_{20}(OH)_4$) and a reference sample of nontronite coded NAu-2 ($(M+_{.97})[Si7_{.57}Al_{.01}Fe_{.42}][Al_{.52}Fe_{3.32}Mg_{.7}]O_{20}(OH)_4$ (Keeling *et al*., 2000)) were used as references to fit the spectra of the unknown. In addition, the Attenuated Total Reflection (ATR) mode (Shimadzu ATR objective Ge prism) was used to obtain FT-IR spectra from the nontronite reference. In addition, the 100 μm thick section was mounted on the stage of the microscope. We attempted to obtain FT-IR spectra from areas associated with the clay-filled fractures using the ATR mode.

https://doi.org/10.1017/S1473550425000011 Published online by Cambridge University Press

O-PTIR and Raman spectroscopy

To acquire O-PTIR spectra from the thin section of the rock interior at the submicron resolution, a mIRage infrared microscope (Photothermal Spectroscopy Corp., Santa Barbara, USA) was used in reflectance mode (Cassegrain 40 × objective) with a continuous wave 532 nm laser as probe beam. The pump beam consisting of a tunable QCL device (800–1895 cm^{-1}; 2 cm^{-1} spectral resolution and 10 scans per spectrum) was used to obtain O-PTIR spectra over the mid-IR ranges. Raman spectra were collected from 4000 to 200 cm^{-1} with 1 s integration and 20 scans for averaging. For microbiological references, co-cultured cells of Nanoarchaeota strain MJ1 and *Metallosphaera* sp. strain MJ1HA (JCM33617) and cultured cells of *Escherichia coli* (NBRC13168) were freeze-dried. The cultured cells, the reference clay samples and a powder of LR White resin were mounted on a CaF_2 disk for analysis.

Results

Conventional FT-IR microscopy for the rock core sample

We collected FT-IR spectra from the clay-sized fractions of U1365E-8R4 and smectite references with a conventional FT-IR microscope with the transmission mode (Fig. 1). In smectite spectra from a 10 µm

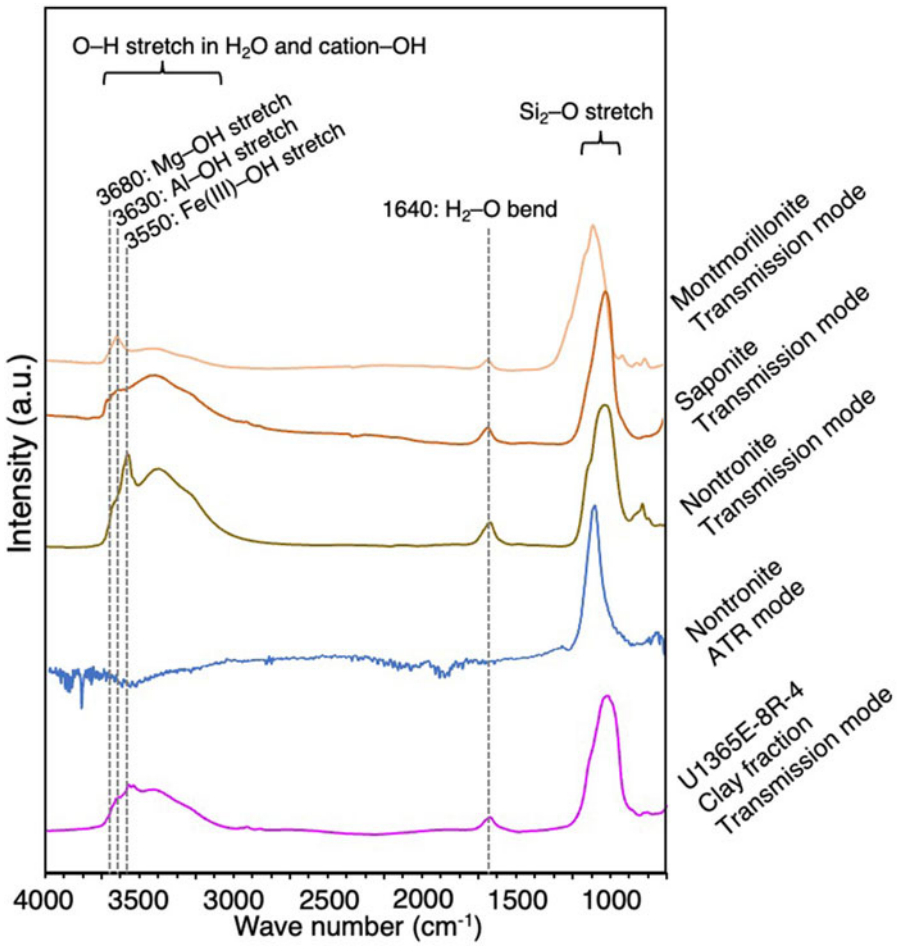

Figure 1. *FT-IR microscopy spectra from smectite references and the clay fraction of the rock core. Peak attributions are described in the text.*

https://doi.org/10.1017/S1473550425000011 Published online by Cambridge University Press

square region, there is a broad peak centred around 3390 cm^{-1}, which is attributed to vibration modes of interlayer H_2O (Bishop *et al.*, 1994; Madejová *et al.*, 1994). A peak at ~1000 cm^{-1} is attributed to Si_2-O symmetric and asymmetric stretching modes (Ellerbrock *et al.*, 2022). Between 3700 and 3550 cm^{-1}, peak and shoulder features are diagnostic to types of cation-OH stretching modes. The $Fe(III)_2$-OH stretching mode has a peak feature at 3550 cm^{-1}(Gates, 2005), whereas well-defined shoulder features at 3630 and 3680 cm^{-1} are attributed to the Al_2–OH and Mg_2–OH stretching modes (Grauby *et al.*, 1993, 1994). FT-IR spectra were similar between U1365E-8R4 and nontronite. The ATR mode was used to obtain FT-IR spectra from the nontronite reference under the same conditions for the transmission mode. The FT-IR spectra have low signal-to-noise ratios with a major peak at ~1000 cm^{-1} shifted towards the higher wavenumber than that obtained from the same reference by the transmission mode (Fig. 1). In addition, a peak attributed to the H_2O bending mode at 1635 cm^{-1} and peaks between 3700 and 3550 cm^{-1} diagnostic to smectite were absent in the spectra. As for the thin section, FT-IR spectra diagnostic to smectite and microbial cells were not obtained (data not shown). FT-IR spectra for microbial cells were not obtained via the ATR mode presumably because of the limitation spatial resolution.

O-PTIR spectroscopy for mapping signals from microbes and smectite

For the thin section of the rock core, O-PTIR spectroscopy was used to map the signal intensities of 1000 and 1530 cm^{-1}, at which major peaks of smectites and microbial cells were respectively obtained (Fig. 2(a)–(e)). At the brownish rim of a greenish fracture made of a Fe-rich mica mineral called celadonite (Fig. 2(a)–(c)), both signal intensities were high (Fig. 2(c)–(e), pink and light blue points), indicating the co-occurrence of smectites and microbial cells.

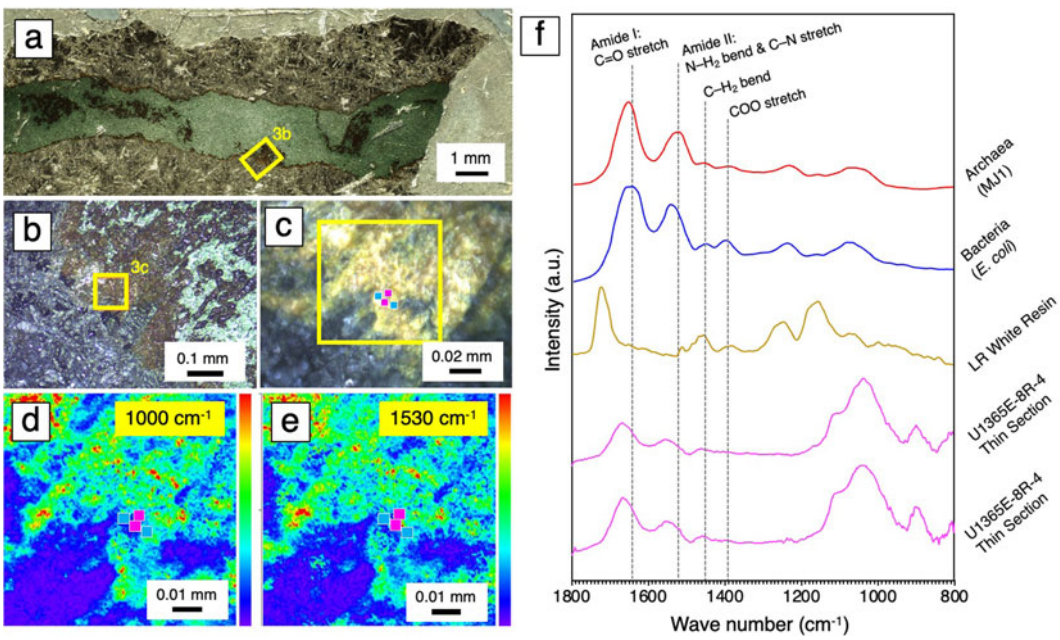

Figure 2. *Photographs of a nontronite-bearing fracture in the thin section from the rock core interior (a–c) with increasing magnification. Intensity maps of optical photothermal infrared (O-PTIR) spectra in a region highlighted with a yellow square in Fig. 2c at 1000 cm^{-1} (d) and 1530 cm^{-1}(e). O-PTIR spectra from duplicate analyses of pink points in Fig.. 2(c)–(e), co-cultured cells of Nanoarchaeota strain MJ1 and* Metallosphaera *sp. strain MJ1HA (JCM33617) and cultured cells of* Escherichia coli *(NBRC13168) and LR White resin (f). Peak assignment was based on Movasaghi* et al. *(2008) and Ellerbrock* et al. *(2022) and references therein.*

https://doi.org/10.1017/S1473550425000011 Published online by Cambridge University Press

O-PTIR spectroscopy for diagnostic spectra from microbes

In O-PTIR spectra obtained from loci with the high signal intensity at 1530 cm^{-1}, peaks attributed to amide I and II (an indicator of peptides) were evident, in addition to a peak at 1450 cm^{-1} attributed to the bending vibration (scissoring) of CH_2 groups in lipids and a peak band at 1390 cm^{-1} attributed to the stretching vibration of COO of amino acid side chains and fatty acids (Lima *et al*., 2021). The spectra were similar to microbial cells but distinct from that from LR White resin (Fig. 2f). It should be noted that the sample damage was not evident during the repeated measurements by O-PTIR.

O-PTIR spectroscopy for diagnostic spectra from smectite

In O-PTIR spectra from 800 to 1800 cm^{-1}, Fe(III)-bearing smectites exhibit a pair of bands at 815–817 and 870 cm^{-1} attributed to the $Fe(III)_2$–OH and the Fe(III)–Al–OH bending modes (Grauby *et al*., 1994; Gates, 2005; Andrieux and Petit, 2010). In addition, a peak attributed to the H_2O bending mode occurs at 1635 cm^{-1} (Bishop *et al*., 1994; Madejová *et al*., 1994). From the thin section of U1365E-8R4, an O-PTIR spectrum similar to that of nontronite was obtained at the points with and without the peaks attributed to Amide I and II (Fig. 3), except for a peak attributed to the Fe(III)–Al–OH bending mode at 870 cm^{-1}.

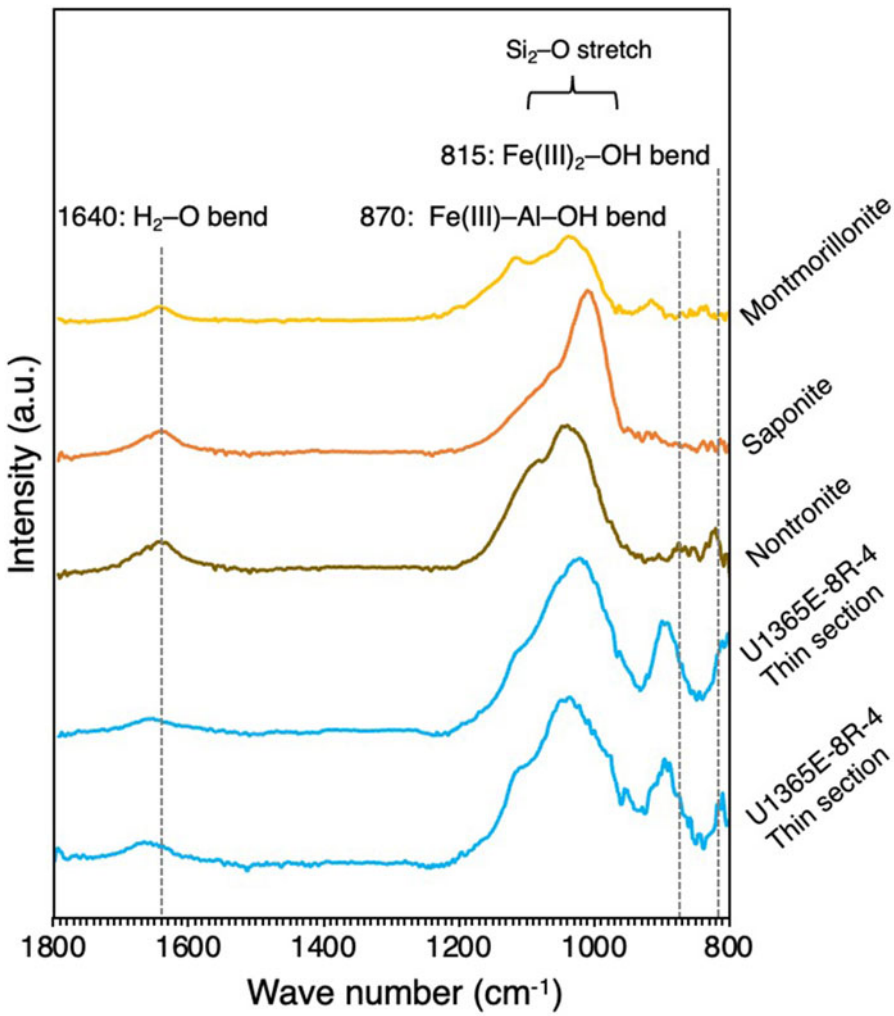

Figure 3. *Duplicate optical photothermal infrared (O-PTIR) spectra of light blue points in Fig. 2(c)–(e) and smectite references. Peak attributions are described in the text.*

https://doi.org/10.1017/S1473550425000011 Published online by Cambridge University Press

μ-Raman spectroscopy for comparison with O-PTIR spectroscopy

We used μ-Raman spectroscopy with an excitation wavelength of 532 nm to obtain spectra from the same spots (Fig. 4), from which O-PTIR spectra identical to nontronite were obtained (Fig. 3). No obvious peaks were present in the Raman spectra (Fig. 4). Next, Raman spectra were obtained from the bacterial culture and the same spots (Fig. 4), from which O-PTIR spectra including sharp amide peaks were obtained (Fig. 2). No obvious peaks were obtained from the bacterial culture and the spots due to the interference by autofluorescence.

Discussion

O-PTIR sensitivity for detecting microbial cells and adjacent smectites from an analogue rock sample

On Mars, basaltic lava is ubiquitous, where Fe- and Mg-bearing smectites with compositions ranging from nontronite (iron endmember) to saponite (magnesium endmember) are the most common clay minerals formed by silicate weathering or hydrothermal alteration (Mustard *et al.*, 2008; Ehlmann

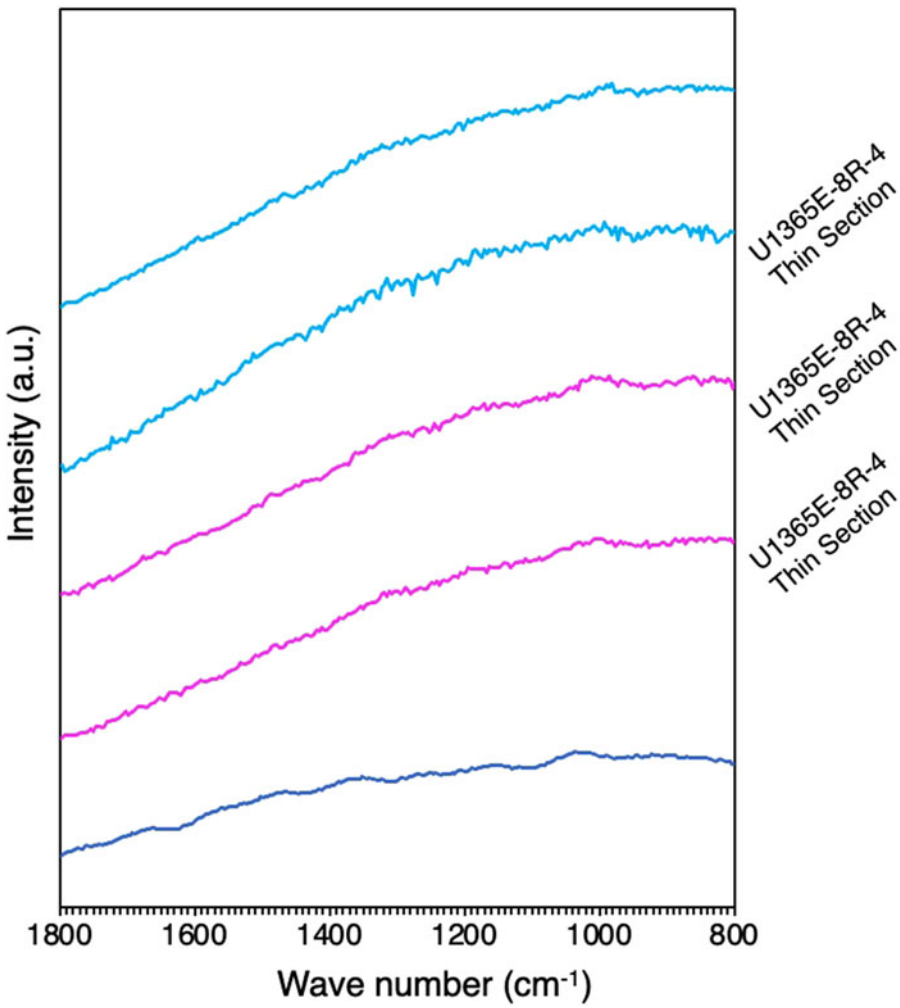

Figure 4. *Raman spectra from light blue and pink points shown in Fig 2(c)–(e) and cultured cells of* Escherichia coli *(NBRC13168).*

https://doi.org/10.1017/S1473550425000011 Published online by Cambridge University Press

et al., 2011). Fe, Mg-rich smectites are similarly observed in settings associated with basaltic lava on Earth (Alt, 1988; Teagle *et al*., 1996; Yamashita *et al*., 2019). We regard the rock core sample drilled from ancient basaltic lava as an analogue rock sample, given that basaltic rock fractures are filled with nontronite.

In our previous studies, a conventional X-ray diffraction analysis was performed using clay-sized fractions separated from crushed rock samples (Sueoka *et al*., 2019; Yamashita *et al*., 2019). In addition, ~100 µm thick sections made from the same core samples by embedding the fracture-bearing rock piece in hydrophilic resin called LR White were subjected to clay mineral characterization using scanning electron microscopy coupled with energy-dispersive spectroscopy (SEM-EDS) and µ-Raman spectroscopy. From regions in the thin section with EDS spectra similar to nontronite, no peaks were obtained in Raman spectra in our previous study (Yamashita *et al*., 2019). Thus, transmission electron microscopy equipped with EDS (TEM-EDS) analysis was necessary for the nanoscale mineralogical identification of nontronite.

Greenish signals from microbial cells stained with SYBR-Green I in the thin sections were visualized by fluorescence microscopy before SEM-EDS analysis was performed for the clay mineral characterization (Suzuki *et al*., 2020). Then, microbial cells in the thin sections were characterized by µ-Raman spectroscopy (Suzuki *et al*., 2020) (Fig. 5). However, fluorescence signals obscured peaks from Raman shifts from the DNA-stained microbial cells (Suzuki *et al*., 2020). To confirm if the greenish signals are originated from microbial cells, nanoscale secondary ion mass spectrometry (NanoSIMS) was used for submicron-scale mapping of carbon, nitrogen, sulphur and phosphorous.

However, it was necessary to fabricate thin sections with a thickness of ~3 µm using a focused ion beam (FIB). To identify minerals around microbial cells, FIB sections needed to be thinned down to a thickness of 100 nm for TEM-EDS. The higher the spatial resolution, the more damaged the sample. Nevertheless, high-resolution analytical data were crucial to determine mineral identity and the biogenicity of signals from SYBR-Green I.

From the rock fracture, we obtained the O-PTIR spectra identical to those from microbial cultures (Fig. 2). These results are consistent with those obtained by NanoSIMS analysis of the FIB-fabricated section (Fig. 5a). The presence of a Fe(III)-Al-OH bend in the O-PTIR spectra adjacent to those of microbial cells is also consistent with TEM-EDS data showing the high Al content in nontronite in the rock fracture (Yamashita *et al*., 2019). The in-situ capability of O-PTIR spectroscopy for

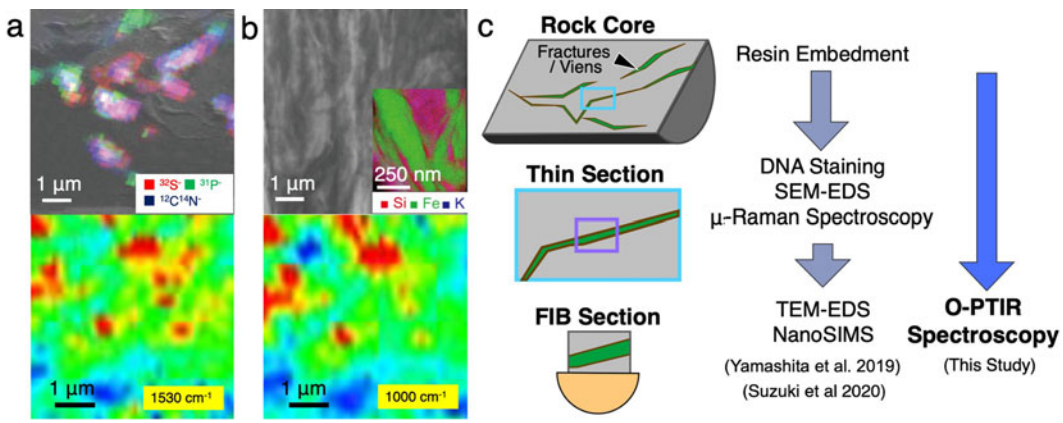

Figure 5. *Comparison of analytical data between NanoSIMS (upper) and O-PTIR (lower) (a) and between TEM-EDS (upper) and O-PITR (lower) (b). Rock characterization procedures performed in our previous and present studies (c). NanoSIMS and TEM-EDS data are modified from Suzuki* et al. *(2020) and Yamashita* et al. *(2019), respectively. SEM, scanning electron microscopy; EDS, energy-dispersive x-ray spectroscopy; FIB, focused ion beam; TEM, transmission electron microscopy; NanoSIMS, nanoscale secondary ion mass spectrometry; O-PTIR, optical-photothermal infrared.*

https://doi.org/10.1017/S1473550425000011 Published online by Cambridge University Press

identifying smectites is also comparable to the high-resolution analyses by TEM-EDS (Fig. 5b). Thus, O-PTIR spectroscopy can be used for detecting microbial cells and smectite, without using our previous published procedures (Fig. 5c). TEM and NanoSIMS are used to resolve cellular ultrastructures (Wanger *et al*., 2012) and to provide ppm-level elemental abundances and isotopic ratios (Ito and Messenger, 2008, 2016), respectively. Therefore, O-PTIR is a good complimentary technique but not a total substitute.

Considerations for the usage of O-PTIR spectroscopy in SRF

Analytical instruments required by sample safety assessment and basic characterization, preliminary examination and time- and sterilization-sensitive sciences are environmental SEM and deep ultraviolet (DUV) fluorescence microscopy/μ-Raman spectroscopy (Carrier *et al*., 2022; Tait *et al*., 2022; Tosca *et al*., 2022; Velbel *et al*., 2022), partly because these analytical instruments are non- or minimally destructive without any sample preparation prior to the analyses. The Mars 2020 Perseverance rover is currently investigating the Noachian Jezero crater, where fine-grained basaltic igneous rocks within the Máaz and Séítah formations were analysed by SHERLOC (Scanning Habitable Environments with Raman and Luminescence for Organics and Chemicals), a DUV fluorescence/Raman spectrometer (Scheller *et al*., 2022; Corpolongo *et al*., 2023; Sharma *et al*., 2023), among other instruments (Udry *et al*., 2022; Beyssac *et al*., 2023; Simon *et al*., 2023). In addition to the structures of biomolecules such as nucleotides and amino acids (Sapers *et al*., 2019), DUV fluorescence/Raman spectroscopy is particularly sensitive to aromatic organic compounds (Abbey *et al*., 2017 and references therein), and its use on Mars has suggested the presence of organic matter on Mars (Scheller *et al*., 2022; Sharma *et al*., 2023). With respect to minerals, some mineral classes (e.g., sulphate vs carbonate and pyroxene vs olivine) are identified by DUV fluorescence/Raman spectroscopy based on the number of major peaks and their general positions in Raman spectra (Hollis *et al*., 2021; Corpolongo *et al*., 2023). However, measurable Raman signals are not obtained from a number of silicate minerals including smectites and iron-rich minerals due to significant UV absorption.

Depending on translucency, FT-IR spectroscopy also listed by SSAF and MSPG2 requires a sample thickness ranging from 10 to 30 μm under transmission mode, which often requires destructive sample preparation. FT-IR microscopy has been applied to detect biological materials from basaltic rock core samples obtained by scientific ocean drilling (Preston *et al*., 2011; Türke *et al*., 2018). In these studies, the 30 μm-thick sections of the rock core samples were prepared (Preston *et al*., 2011; Türke *et al*., 2018). Destructive sample preparation required for the transmission mode of FT-IR microscopy is not necessary for the ATR mode. As previously demonstrated (Tanykova *et al*., 2021), the absorption intensities of FT-IR spectra by the ATR mode are substantially lower than those by the transmission mode. Although this study attempted to obtain FT-IR spectra via the ATR mode, no FT-IR spectra diagnostic to microbial cells or smectite were obtained.

The in-situ capability of O-PTIR spectroscopy to sensitively identify smectites has some advantage over those of DUV fluorescence/Raman spectroscopy and FT-IR microscopy, given that Fe/Mg smectites, one of the most widely reported hydrated minerals on Mars including the Jezero crater, are known for preservation of organic biosignatures (Singh *et al*., 2022). In particular, the high spatial resolution and negligible interferences for the detection of organics with high structural complexity such as peptides and smectites are crucial to obtain the co-occurrence pattern, as well as the abiotic background associated with smectites.

After spectroscopic analyses, the SSAF test sequence suggests destructive analyses using organic extracts (Kminek *et al*., 2022a). Mass spectrometers and next-generation DNA sequencers are proposed to detect biomolecules expected in terrestrial life. Martian life could use biomolecules other than nucleic acids, proteins and lipids, on which the methodology of terrestrial life detection is based. Thus, even if no biomolecules known from terrestrial life are detected, agnostic life detection targeting non-terrestrial life will be necessary. If non-terrestrial life occurs in Mars return samples, O-PTIR spectroscopy can detect some characteristics of Martian life such as the enrichment of organic molecules

https://doi.org/10.1017/S1473550425000011 Published online by Cambridge University Press

with sufficient structural complexity unexplained by known abiotic processes. In addition, the space and cost required for O-PTIR spectroscopy are comparable to those required for DUV fluorescence/ Raman spectroscopy.

Acknowledgments. We are grateful to Takahiro Tajima and Yasushi Suzuki from Shimadzu Corporation and Hanae Kobayashi from Nihon Thermal Consulting Co., Ltd. for their technical assistance about FT-IR microscopy and O-PTIR spectroscopy, respectively. Y. S. was supported by the Astrobiology Center Program of National Institutes of Natural Sciences (NINS) (AB0502). M. A. S. was supported by UK Space Agency grants ST/V002732/1 and ST/V006134/1.

Competing interests. The authors declare that the research was conducted in the absence of any commercial or financial relationships that could be construed as a potential conflict of interest.

References

Abbey WJ, Bhartia R, Beegle LW, DeFlores L, Paez V, Sijapati K, Sijapati S, Williford K, Tuite M, Hug W and Reid R (2017) Deep UV Raman spectroscopy for planetary exploration: the search for in situ organics. *Icarus* **290**, 201–214.

Alt JC (1988) Hydrothermal oxide and nontronite deposits on seamounts in the eastern Pacific. *Marine Geology* **81**, 227–239.

Andrieux P and Petit S (2010) Hydrothermal synthesis of dioctahedral smectites: the Al–Fe^{3+} chemical series Part I: influence of experimental conditions. *Applied Clay Science* **48**, 5–17.

Beyssac O, Forni O, Cousin A, Udry A, Kah LC, Mandon L, Clavé E, Liu Y, Poulet F, Quantin Nataf C, Gasnault O, Johnson J, Benzerara K, Beck P, Dehouck E, Mangold N, Alvarez Llamas C, Anderson R, Arana G, Barnes R, Bernard S, Bosak T, Brown AJ, Castro K, Chide B, Clegg S, Cloutis E, Fouchet T, Gabriel T, Gupta S, Lacombe G, Lasue J, Le Mouelic S, Lopez-Reyes G, Madariaga JM, McCubbin FM, McLennan S, Manrique JA, Meslin PY, Montmessin F, Núñez J, Ollila AM, Ostwald A, Pilleri P, Pinet P, Royer C, Sharma SK, Schröder S, Simon JI, Toplis MJ, Veneranda M, Willis PA, Maurice S and Wiens RC (2023) Petrological traverse of the olivine cumulate Séítah formation at Jezero crater, Mars: a perspective from SuperCam onboard Perseverance. *Journal of Geophysical Research Planets* **128**, e2022JE007638.

Bishop JL, Pieters CM and Edwards JO (1994) Infrared spectroscopic analyses on the nature of water in montmorillonite. *Clays and Clay Minerals* **42**, 702–716.

Carrier BL, Beaty DW, Hutzler A, Smith AL, Kminek G, Meyer MA, Haltigin T, Hays LE, Agee CB, Busemann H, Cavalazzi B, Cockell CS, Debaille V, Glavin DP, Grady MM, Hauber E, Marty B, McCubbin FM, Pratt LM, Regberg AB, Smith CL, Summons RE, Swindle TD, Tait KT, Tosca NJ, Udry A, Usui T, Velbel MA, Wadhwa M, Westall F and Zorzano M-P (2022) Science and curation considerations for the design of a Mars Sample Return (MSR) Sample Receiving Facility (SRF). *Astrobiology* **22**, S217–S237.

Corpolongo A, Jakubek RS, Burton AS, Brown AJ, Yanchilina A, Czaja AD, Steele A, Wogsland B, Lee C, Flannery D, Baker D, Cloutis E, Cardarelli EL, Scheller EL, Berger EL, McCubbin FM, Razzell Hollis J, Hickman-Lewis K, Steadman K, Uckert K, DeFlores L, Kah LC, Beegle LW, Fries M, Minitti M, Haney NC, Conrad P, Morris RV, Bhartia R, Roppel RD, Siljeström S, Asher SA, Bykov SV, Sharma S, Shkolyar S, Fornaro T and Abbey WJ (2023) SHERLOC Raman mineral class detections of the Mars 2020 Crater Floor Campaign. *Journal of Geophysical Research Planets* **128**, e2022JE007455.

D'Hondt S, Inagaki F, Zarikian C, Abrams K, Dubois N, Engelhardt T, Evans H, Ferdelman T, Gribsholt B, Harris R, Hoppie B, Hyun J-H, Kallmeyer J, Kim J, Lynch J, McKinley C, Mitsunobu S, Morono Y, Murray R, Pockalny R, Sauvage J, Shimono T, Shiraishi F, Smith D, Smith-Duque C, Spivack A, Steinsbu B, Suzuki Y, Szpak M, Toffin L, Uramoto G, Yamaguchi Y, Zhang G-L, Zhang X-H and Ziebis W (2015) Presence of oxygen and aerobic communities from sea floor to basement in deep-sea sediments. *Nature Geoscience* **8**, 299–304.

Ehlmann BL, Mustard JF, Murchie SL, Bibring J-P, Meunier A, Fraeman AA and Langevin Y (2011) Subsurface water and clay mineral formation during the early history of Mars. *Nature* **479**, 53–60.

Ellerbrock R, Stein M and Schaller J (2022) Comparing amorphous silica, short-range-ordered silicates and silicic acid species by FTIR. *Scientific Reports* **12**, 11708.

Gates W (2005) Infrared spectroscopy and the chemistry of dioctahedral smectites. In Kloprogge JT (ed.), *CMS Workshop Lectures*, vol. **13**. Evergreen, CO: Clay Minerals Society, pp. 125–168.

Grauby O, Petit S, Decarreau A and Baronnet A (1993) The beidellite-saponite series: an experimental approach. *European Journal of Mineralogy* **5**, 623–636.

Grauby O, Petit S, Decarreau A and Baronnet A (1994) The nontronite-saponite series: an experimental approach. *The Journal of Mineralogy* **6**, 99–112.

Haltigin T, Hauber E, Kminek G, Meyer MA, Agee CB, Busemann H, Carrier BL, Glavin DP, Hays LE and Marty B (2022) Rationale and proposed design for a Mars Sample Return (MSR) science program. *Astrobiology* **22**, S27–S56.

Hollis JR, Abbey W, Beegle LW, Bhartia R, Ehlmann BL, Miura J, Monacelli B, Moore K, Nordman A and Scheller E (2021) A deep-ultraviolet Raman and fluorescence spectral library of 62 minerals for the SHERLOC instrument onboard Mars 2020. *Planetary and Space Science* **209**, 105356.

Ito M and Messenger S (2008) Isotopic imaging of refractory inclusions in meteorites with the NanoSIMS 50L. *Applied Surface Science* **255**, 1446–1450.

Ito M and Messenger S (2016) Rare earth element measurements and mapping of minerals in the Allende CAI, 7R19-1, by Nano SIMS ion microprobe. *Meteoritics & Planetary Science* **51**, 818–832.

Keeling JL, Raven MD and Gates WP (2000) Geology and characterization of two hydrothermal nontronites from weathered metamorphic rocks at the Uley graphite mine, South Australia. *Clays and Clay Minerals* **48**, 537–548.

Kminek G, Benardini JM, Brenker FE, Brooks T, Burton AS, Dhaniyala S, Dworkin JP, Fortman JL, Glamoclija M, Grady MM, Graham HV, Haruyama J, Kieft TL, Koopmans M, McCubbin FM, Meyer MA, Mustin C, Onstott TC, Pearce Z, Pratt LM, Sephton MA, Siljeström S, Sugahara H, Suzuki S, Suzuki Y, Zuilen M and Viso M (2022a) COSPAR sample safety assessment framework (SSAF). *Astrobiology* **22**, S186–S216.

Kminek G, Meyer MA, Beaty DW, Carrier BL, Haltigin T and Hays LE (2022b) Mars sample Return (MSR): planning for returned sample science. *Astrobiology* **22**, S1–S4.

Li X, Zhang D, Bai Y, Wang W, Liang J and Cheng JX (2019) Fingerprinting a living cell by Raman integrated mid-infrared photothermal microscopy. *Analytical Chemistry* **91**, 10750–10756.

Lima C, Muhamadali H, Xu Y, Kansiz M and Goodacre R (2021) Imaging isotopically labeled bacteria at the single-cell level using high-resolution optical infrared photothermal spectroscopy. *Analytical Chemistry* **93**, 3082–3088.

Madejová J, Komadel P and Čičel B (1994) Infrared study of octahedral site populations in smectites. *Clay Minerals* **29**, 319–326.

Meyer MA, Kminek G, Beaty DW, Carrier BL, Haltigin T, Hays LE, Agree CB, Busemann H, Cavalazzi B, Cockell CS, Debaille V, Glavin DP, Grady MM, Hauber E, Hutzler A, Marty B, McCubbin FM, Pratt LM, Regberg AB, Smith AL, Smith CL, Summons RE, Swindle TD, Tait KT, Tosca NJ, Udry A, Usui T, Velbel MA, Wadhwa M, Westall F and Zorzano M-P (2022) Final report of the Mars Sample Return Science Planning Group 2 (MSPG2). *Astrobiology* **22**, S5–S26.

Morono Y, Ito M, Hoshino T, Terada T, Hori T, Ikehara M, D'Hondt S and Inagaki F (2020) Aerobic microbial life persists in oxic marine sediment as old as 101.5 million years. *Nature Communications* **11**, 1–9.

Movasaghi Z, Rehman S and Rehman DI (2008) Fourier transform infrared (FTIR) spectroscopy of biological tissues. *Applied Spectroscopy Review* **43**, 134–179.

Mustard JF, Murchie SL, Pelkey S, Ehlmann B, Milliken R, Grant JA, Bibring JP, Poulet F, Bishop J, Dobrea EN, Roach L, Seelos F, Arvidson RE, Wiseman S, Green R, Hash C, Humm D, Malaret E, McGovern JA, Seelos K, Clancy T, Clark R, Marais DD, Izenberg N, Knudson A, Langevin Y, Martin T, McGuire P, Morris R, Robinson M, Roush T, Smith M, Swayze G, Taylor H, Titus T and Wolff M (2008) Hydrated silicate minerals on Mars observed by the Mars Reconnaissance Orbiter CRISM instrument. *Nature* **454**, 305–309.

Onstott TC, Ehlmann BL, Sapers H, Coleman M, Ivarsson M, Marlow JJ, Neubeck A and Niles P (2019) Paleo-rock-hosted life on Earth and the search on Mars: a review and strategy for exploration. *Astrobiology* **19**, 1230–1262.

Preston L, Izawa M and Banerjee N (2011) Infrared spectroscopic characterization of organic matter associated with microbial bioalteration textures in basaltic glass. *Astrobiology* **11**, 585–599.

Sapers HM, Razzell Hollis J, Bhartia R, Beegle LW, Orphan VJ and Amend JP (2019) The cell and the sum of its parts: patterns of complexity in biosignatures as revealed by deep UV Raman spectroscopy. *Frontiers in Microbiology* **10**, 679.

Scheller EL, Razzell Hollis J, Cardarelli EL, Steele A, Beegle LW, Bhartia R, Conrad P, Uckert K, Sharma S, Ehlmann BL, Abbey WJ, Asher SA, Benison KC, Berger EL, Beyssac O, Bleefeld BL, Bosak T, Brown AJ, Burton AS, Bykov SV, Cloutis E, Fairén AG, DeFlores L, Farley KA, Fey DM, Fornaro T, Cox AC, Fries M, Hickman-Lewis K, Hug WF, Huggett JE, Imbeah S, Jakubek RS, Kah LC, Kelemen P, Kennedy MR, Kizovski T, Lee C, Liu Y, Mandon L, McCubbin FM, Moore KR, Nixon BE, Nuñez JI, Rodriguez Sanchez-Vahamonde C, Roppel RD, Schulte M, Sephton MA, Sharma SK, Siljestrom S, Shkolyar S, Shuster DL, Simon JI, Smith RJ, Stack KM, Steadman K, Weiss BP, Werynski A, Williams AJ, Wiens RC, Williford KH, Winchell K, Wogsland B, Yanchilina A, Yingling R and Zorzano M-P (2022) Aqueous alteration processes in Jezero crater, Mars – implications for organic geochemistry. *Science* **378**, 1105–1110.

Sharma S, Roppel RD, Murphy AE, Beegle LW, Bhartia R, Steele A, Razzell Hollis J, Siljeström S, McCubbin FM, Asher SA, Abbey WJ, Allwod AC, Berger EL, Bleefeld BL, Burton AS, Bykov SV, Cardarelli EL, Conrad P, Corpolongo A, Czaja AD, DeFlores L, Edgett K, Farley KA, Fornaro T, Fox AC, Fries M, Harker D, Hickman-Lewis K, Huggett JE, Imbeah S, Jakubek RS, Kah LC, Lee C, Liu Y, Magee A, Minitti M, Moore KR, Pascuzzo A, Rodriguez C, Scheller EL, Shkolyar S, Stack KM, Steadman K, Tuite M, Uckert K, Werynski A, Wiens RC, Williams AJ, Winchell K, Wu M and Yanchilina A (2023) Diverse organic-mineral associations in Jezero crater, Mars. *Nature* **619**, 724–732.

Simon JI, Hickman-Lewis K, Cohen BA, Mayhew LE, Shuster DL, Debaille V, Hausrath EM, Weiss BP, Bosak T, Zorzano M-P, Amundsen HEF, Beegle LW, Bell III JF, Benison KC, Berger EL, Beyssac O, Brown AJ, Calef F, Casademont TM, Clark B, Clavé E, Crumpler L, Czaja AD, Fairén AG, Farley KA, Flannery DT, Fornaro T, Forni O, Gómez F, Goreva Y, Gorin A, Hand KP, Hamran S-E, Henneke J, Herd CDK, Horgan BHN, Johnson JR, Joseph J, Kronyak RE, Madariaga JM, Maki JN, Mandon L, McCubbin FM, McLennan SM, Moeller RC, Newman CE, Núñez JI, Pascuzzo AC, Pedersen DA, Poggiali G, Pinet P, Quantin-Nataf C, Rice M, Rice Jr JW, Royer C, Schmidt M, Sephton M, Sharma S, Siljeström S, Stack KM, Steele A, Sun VZ, Udry A, VanBommel S, Wadhwa M, Wiens RC, Williams AJ and Williford KH (2023) Samples collected from the floor of Jezero Crater with the Mars 2020 Perseverance Rover. *Journal of Geophysical Research: Planets* **128**, e2022JE007474.

Singh D, Sinha RK, Singh P, Roy N and Mukherjee S (2022) Astrobiological potential of Fe/Mg smectites with special emphasis on Jezero Crater, Mars 2020 landing site. *Astrobiology* **22**, 579–597.

Sueoka Y, Yamashita S, Kouduka M and Suzuki Y (2019) Deep microbial colonization in saponite-bearing fractures in aged basaltic crust: implications for subsurface life on Mars. *Frontiers in Microbiology* **10**, 2793.

Suzuki Y, Yamashita S, Kouduka M, Ao Y, Mukai H, Mitsunobu S, Kagi H, D'Hondt S, Inagaki F and Morono Y (2020) Deep microbial proliferation at the basalt interface in 33.5–104 million-year-old oceanic crust. *Communications Biology* **3**, 136.

Tait KT, McCubbin FM, Smith CL, Agee CB, Busemann H, Cavalazzi B, Debaille V, Hutzler A, Usui T and Kminek G (2022) Preliminary planning for Mars Sample Return (MSR) curation activities in a Sample Receiving Facility (SRF). *Astrobiology* **22**, S57–S80.

Tanykova N, Petrova Y, Kostina J, Kozlova E, Leushina E and Spasennykh M (2021) Study of organic matter of unconventional reservoirs by IR spectroscopy and IR microscopy. *Geosciences* **11**, 277.

Teagle DA, Alt JC, Bach W, Halliday AN and Erzinger J (1996) Alteration of upper ocean crust in a ridge-flank hydrothermal upflow zone: mineral, chemical, and isotopic constraints from Hole 896A. *Proceedings of the Ocean Drilling Program, Scientific Results* **148**, 119–150.

Udry A, Ostwald A, Sautter V, Cousin A, Beyssac O, Forni O, Dromart G, Benzerara K, Nachon M, Horgan B, Mandon L, Clavé E, Dehouck E, Gibbons E, Alwmark S, Ravanis E, Wiens RC, Legett C, Anderson R, Pilleri P, Mangold N, Schmidt M, Liu Y, Núñez JI, Castro K, Madariaga JM, Kizovski T, Beck P, Bernard S, Bosak T, Brown A, Clegg S, Cloutis E, Cohen B, Connell S, Crumpler L, Debaille V, Flannery D, Fouchet T, Gabriel TSJ, Gasnault O, Herd CDK, Johnson J, Anrique JA, Maurice S, McCubbin FM, McLennan S, Ollila A, Pinet P, Quantin-Nataf C, Royer C, Sharma S, Simon JI, Steele A, Tosca N, Treiman A and the SuperCam team (2022) A Mars 2020 perseverance SuperCam perspective on the igneous nature of the Máaz formation at Jezero crater and link with Séítah, Mars. *Journal of Geophysical Research: Planets* **127**, e2022JE007440.

Tosca NJ, Agee CB, Cockell CS, Glavin DP, Hutzler A, Marty B, McCubbin FM, Regberg AB, Velbel MA and Kminek G (2022) Time-sensitive aspects of Mars Sample Return (MSR) science. *Astrobiology* **22**, S81–S111.

Türke A, Ménez B and Bach W (2018) Comparing biosignatures in aged basalt glass from North Pond, Mid-Atlantic Ridge and the Louisville Seamount Trail, off New Zealand. *PLoS ONE* **13**, e0190053.

Velbel MA, Cockell CS, Glavin DP, Marty B, Regberg AB, Smith AL, Tosca NJ, Wadhwa M, Kminek G and Meyer MA (2022) Planning implications related to sterilization-sensitive science investigations associated with Mars Sample Return (MSR). *Astrobiology* **22**, S112–S164.

Wanger G, Moser D, Hay M, Myneni S, Onstott TC and Southam G (2012) Mobile hydrocarbon microspheres from >2-billion-year-old carbon-bearing seams in the South African deep subsurface. *Geobiology* **10**, 496–505.

Yamashita S, Mukai H, Tomioka N, Kagi H and Suzuki Y (2019) Iron-rich smectite formation in subseafloor Basaltic lava in aged oceanic crust. *Scientific Reports* **9**, 11306.